The Parasagittal Line: An Anatomic Landmark for Axial Imaging

Thomas P. Naidich, Jeffrey T. Blum and Michael I. Firestone

AJNR Am J Neuroradiol 2001, 22 (5) 885-895
http://www.ajnr.org/content/22/5/885

AJNR Am J Neuroradiol 22:885–895, May 2001

The Parasagittal Line: An Anatomic Landmark for Axial Imaging

Thomas P. Naidich, Jeffrey T. Blum, and Michael I. Firestone

BACKGROUND AND PURPOSE: **No validated imaging landmark exists for characterizing the medial-lateral position of abnormalities at the high convexity–parasagittal region. Our understanding of the courses and deflections of the upper cerebral sulci is limited. Our purpose, therefore, was to define a frontooccipital line with reproducible anatomic relations to the upper cerebral gyri and sulci and to validate that line for use as an anatomic landmark by specific analysis of the gyral-sulcal relationships along it.**

METHODS: **In 100 subjects of all ages, the gyri and sulci visualized on serial axial CT sections of the upper brain were traced onto a single flat surface to delineate the anatomic relationships among the midline interhemispheric fissure, the paramedian superior frontal sulci (SFS) and intraoccipital sulci (IOS), the medial surface sulci, the high convexity sulci, and the inner table of the skull. These tracings provided a template for drawing a straight, best-fit parasagittal line from the SFS to the IOS and for assessing how reproducibly key anatomic structures align along the parasagittal line. To assure the applicability of the line to MR imaging, selected relationships were retested on serial axial MR sections in the same subjects.**

RESULTS: **The parasagittal line could be drawn in each case and showed reproducible alignment with the SFS, hand-motor area, partes marginales, pars deflections, postcentral ''parentheses,'' distal intraparietal sulci, and IOS. In supraventricular sections, the parasagittal line separated the sulci arising along the medial surface from those arising along the convexity.**

CONCLUSION: **Because the anatomic relationships of the parasagittal line are reproducible, it may serve as a reference line or landmark. The tendency of this line to demarcate medial sulci from convexity sulci suggests immediate application to the definition of vascular territories and vascular watersheds, a topic under active investigation.**

At present, there is no well-defined anatomic landmark or reference line that is suitable for describing the medial-lateral position and extent of lesions seen on axial CT and MR images. Recent anatomic work has begun to elucidate recognizable patterns among the gyri and sulci of the cerebral hemispheres (1–14), including the hand-motor areas of the precentral gyri (4, 10, 11), the partes marginales of the cingulate sulci (2, 4), the pars deflections (3, 4), the ''parentheses'' formed by the postcentral sulci (4), the subparietal sulci (SPS) (2, 4), the parietooccipital sulci (POS) (4, 5), the intraparietal sulci (IPS) (1, 5), and the intraoccipital sulci (IOS) (1, 4, 5) (Fig 1). A review of normal CT scans suggested that there might also be a reproducible alignment of the gyri and sulci of the medial, parasagittal, and high convexity surfaces of the brain along a frontooccipital vector. This study was undertaken to evaluate a specific parasagittal line hand drawn as a best-fit straight line through the superior frontal sulcus (SFS) anteriorly and the IOS posteriorly. This best-fit line did not necessarily parallel the falx and did not necessarily show mirror-image symmetry with the contralateral parasagittal line, particularly in cases of pronounced parietooccipital asymmetry (petalia) (15).

Received June 13, 2000; accepted after revision July 10.

From the Department of Radiology, The Mount Sinai Medical Center, New York, NY (T.P.N., M.I.F.) and the Department of Radiology, Westside Regional Medical Center, Plantation, FL.

Presented in part at the annual meeting of the American Society of Neuroradiology, San Diego, May 1999.

Address reprint requests to Thomas P. Naidich, MD, Department of Radiology, Box 1234, The Mount Sinai Medical Center, 1 Gustave Levy Place, New York, NY 10029.

Methods

The study population consisted of 100 healthy subjects of all ages in whom both CT and MR studies of the brain were available to review in hard copy. The group consisted of 40 males and 60 females ranging in age from 2 months to 92 years (average age, 46 years). By decade (D) the subjects were distributed as follows: D1, 9%; D2, 9%; D3, 9%; D4, 13%; D5, 13%; D6, 15%; D7, 18%; D8, 10%; D9, 3%; and D10, 1%. Thus, 27% were less than 30 years old and 73% were 30

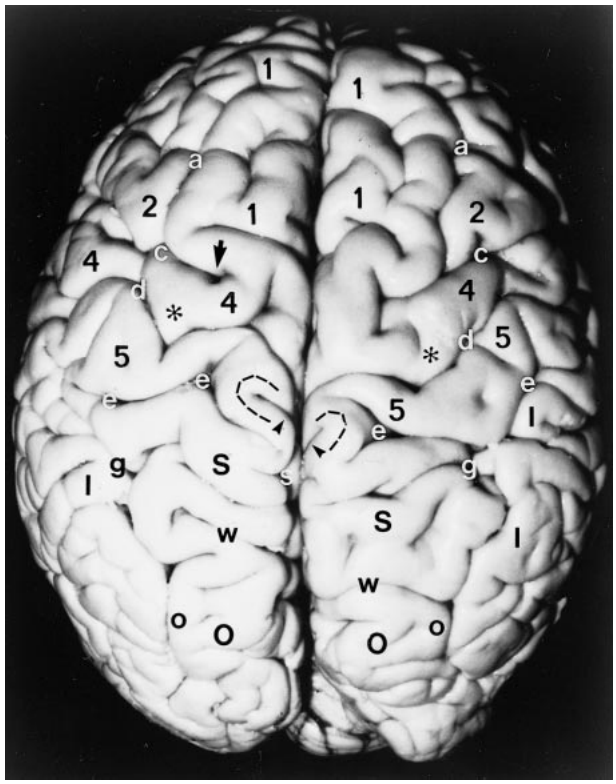

FIG 1. Anatomic specimen. Superior surface of the brain after removal of the pia-arachnoid and surface vasculature. Note the positions, alignments, and interrelationships among the gyri: superior frontal gyrus (*1*), middle frontal gyrus (*2*), precentral gyrus (*4*), postcentral gyrus (*5*), pars deflection (*dashed curve*), superior parietal lobule (*large black S*), inferior parietal lobule (*l*), and superior occipital gyrus (*large O*), and among the sulci: superior frontal sulcus (*a*), precentral sulcus (*c*), central sulcus (*d*), postcentral sulcus (*e*), including the medial parentheses (also *e*), pars marginalis (*arrowheads*), intraparietal sulcus (*g*), subparietal sulcus (*small white s*), parietooccipital sulcus (*w*), and intraoccipital sulcus (*small o*). Note the notch (*arrow*) in the precentral sulcus anterior to the hand-motor area, the sharp inscription of the central sulcus just medial to the knob (*asterisks*) of the hand-motor area, the medial positions of the pars marginalis, SPS and POS, the nesting of the pars deflection (*dashed curve*) between the pars marginalis (*arrowheads*) and the postcentral parenthesis (*e*) on each side, and the convergence of the posterior portions of the IPS toward the parasagittal line.

years old or older. The 100 subjects provided 200 hemispheres for analysis.

In each subject the gyri and sulci visualized on the upper axial CT sections were carefully and systematically traced onto paper to provide a single composite view of the relative positions of the midline interhemispheric fissure and the paired SFS, precentral sulci, central sulci, postcentral sulci (including their superomedial bifurcations to form parentheses), the partes marginalis of the cingulate sulci, the white matter of the pars deflections, the POS, the IPS, and the IOS (which represent the continuations of the IPS posterior to the POS). In each case, the precise position and configuration of the hand-motor areas along the posterior surfaces of the precentral gyri were carefully depicted bilaterally. The positions of any notches in the precentral sulci just anterior to the hand-motor area were also marked in the tracing. Because the structures tested lay in different planes and were not all visible on the same slice, the tracing paper was moved progressively from one imaging section to another to trace the proper position of each structure onto the same flat composite projection. In each section, care was exercised to maintain precise alignment with the image and with the rectangular frame of the image. The best possible straight line was then selected by eye and hand drawn through the SFS and the IOS on each side, directly onto the tracing. This SFS-IOS line was designated the parasagittal line (Fig 2).

The entire series of 100 CT scans was then analyzed to determine the position of each structure with respect to this parasagittal line. Position of a structure within 1.5 mm medial or lateral to the parasagittal line on the hard copy was considered to be ''on'' the line. In our images this corresponded to $\pm$ 4.7 mm in vivo (ie, 1.5 $\times$ 3.1 mm full magnification factor) = $\pm$ 4.65 mm. A narrower criterion of 1.0 mm ($\pm$ 3.1 mm in vivo) was used for the postcentral parenthesis. These ranges of 4.7 mm and 3.1 mm, in vivo, appeared to identify a natural grouping in the study material, since these ranges included nearly all cases but discriminated against a small number of outlying data points. Specific anatomic relationships were then retested by replicating portions of the process on the MR studies of the same 100 subjects (Fig 3).

Results

The parasagittal line could be drawn successfully in each hemisphere (100%). Detailed analysis of the relationships of the parasagittal line to each sulcus is given in Tables 1 and 2. Specifics follow.

Precentral Sulcus (Figs 2–4)

A short deflection or notch is seen in the precentral sulcus just anterior to the hand-motor area, near the junction of the precentral sulcus with the SFS. The precentral notch was identified by CT in 196 (98%) of 200 hemispheres. The precentral notch lay medial to the parasagittal line in one (0.5%) of 200 hemispheres, on the line in 150 hemispheres (75%), and lateral to the line in 45 hemispheres (22.5%). It was not seen in four hemispheres (2%). Defining malaligned as a position greater than 1.5 mm medial to the parasagittal line, then the precentral notch was aligned along or lateral to the line in 97.5% of hemispheres, malaligned in only 0.5% of hemispheres, and not seen in 2% of hemispheres. The precentral notch lay on the parasagittal line bilaterally in 57% of brains. The notch was never positioned medial to the parasagittal line bilaterally (0%).

Hand-Motor Area of the Precentral Gyrus (Figs 2–4)

The hand-motor area was identified by CT bilaterally in all cases (100%). It took the shape of a single, posteriorly directed, knob or omega (ω) in 147 of 200 hemispheres (Fig 4A) and of a double-hump, dual-arc epsilon (ϵ) in 53 of 200 hemispheres (Fig 4B). The distribution of shapes was 69 ω's and 31 ϵ's on the right and 78 ω's and 22 ϵ's on the left. The central sulcus typically exhibited a sharp deflection or inscription at the medial edge of the ω- or ϵ-shaped hand-motor area.

ω-Shaped Hand-Motor Areas (n = 147 Hemispheres).—The parasagittal line typically crossed the precentral gyrus and the central sulcus just medial to the medial edge of the single ω-shaped

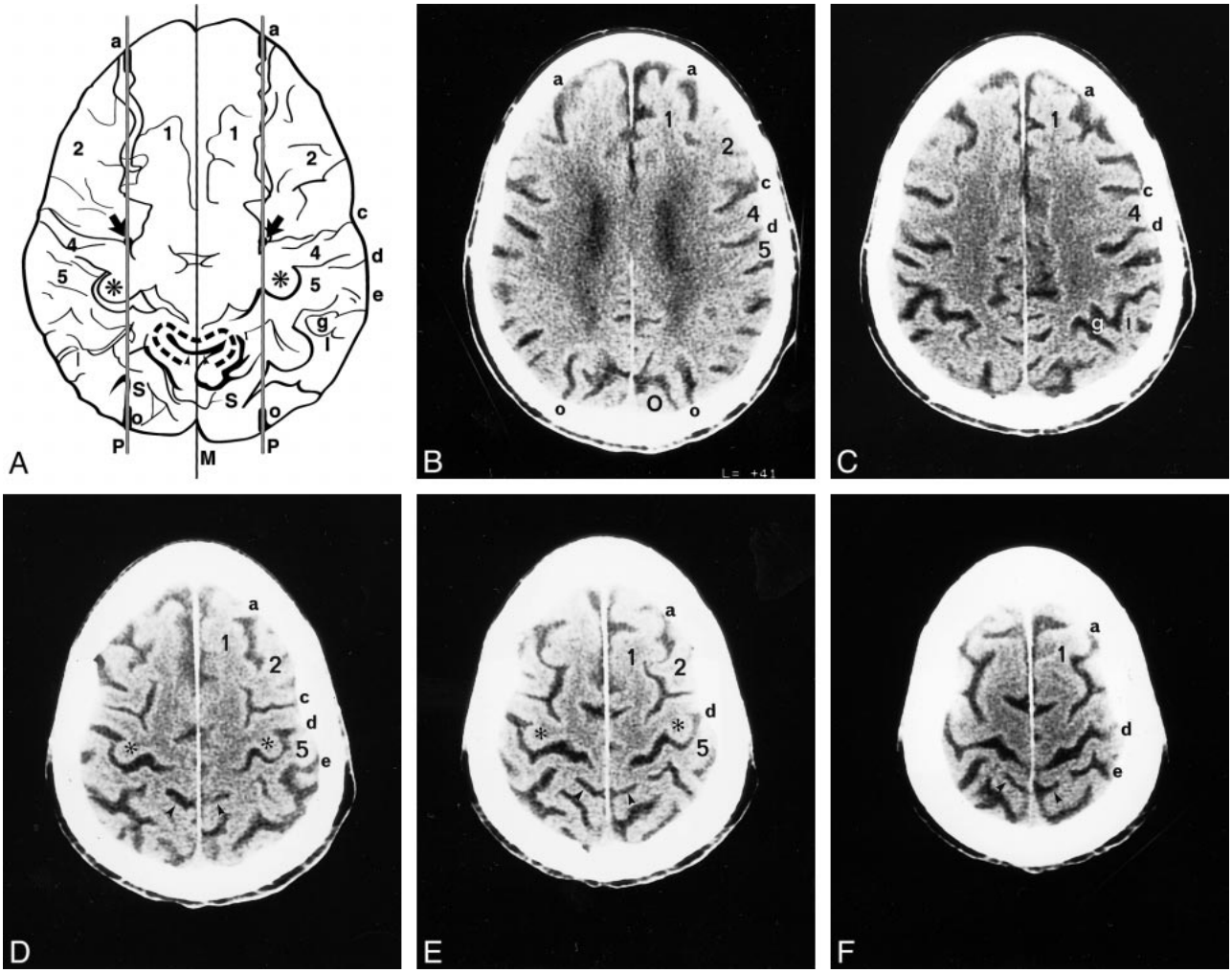

FIG 2. *A–F,* Anatomic relationships of the parasagittal line in a 92-year-old man. The composite representation (*A*) was traced from serial axial CT images (*B–F*). Labels as in Figure 1. *M* indicates midline. In *A,* the *curved gray lines* surrounding the partes marginales (*arrowheads*) represent the pars deflections and correspond to the *dashed curved lines* seen around the partes marginales in Figure 1. In the supraventricular sections, the parasagittal line (paramedian lines, *P*) demarcate the deepest extensions of the medial sulci and separate them from the deepest extensions of the lateral sulci. In the upper sections, multiple transverse sulci show short sharp deflections, which align along the parasagittal line. Note specifically the alignment of the SFS (*a*) and IOS (*o*) along the parasagittal line and their alignment with the notches in the precentral sulci (*arrows*), with the medial aspects of the knobs (*asterisks*) of the hand-motor areas, and with the inscriptions in the central sulci (*d*) just medial to the hand-motor areas. The partes marginales (*arrowheads*), pars deflections (*gray pencil lines*), and postcentral parentheses lie medial to the parasagittal line. In this composite tracing, the inferiorly situated occipital sulci superimpose upon the superior parietal lobules (*S*).

hand-motor area. The medial edge of the hand-motor area lay more than 1.5 mm medial to the parasagittal line in 8.8% of the 147 hemispheres, on the line in 87.1%, and lateral to the line in 4.1%. Defining malaligned as a position greater than 1.5 mm away from the parasagittal line, then the medial edge of the single ω was aligned along the line in 87.1%, malaligned medially in 8.8%, and malaligned laterally in 4.1% of hemispheres.

ϵ-Shaped Hand-Motor Areas (n = 53 Hemispheres).—The parasagittal line crossed through the ϵ-shaped knob of the hand-motor area in 96.2% of these 53 hemispheres. It crossed through the medial arc of the ϵ in 73.6% and crossed the midpoint of the ϵ in an additional 22.6%. The parasagittal line never crossed through the lateral arc of the ϵ. The ϵ-shaped hand-motor area lay wholly lateral to the parasagittal line in 3.8%. Defining malaligned as only the hemispheres in which the parasagittal line crossed through the lateral arc of the ϵ or in which the entire ϵ lay lateral to the line, then the ϵ-shaped hand-motor area was aligned along the line in 96.2% of brains and was malaligned in only 3.8%.

Taking both the ω- and the ϵ-shaped hand-motor areas together, the hand-motor area aligned along the parasagittal line in 89% of right hemispheres and in 90% of left hemispheres. In the others, the malalignment was unilateral in 19 brains and bilateral in one brain.

The Postcentral Parentheses (1.0-mm Criterion) (Figs 2–4)

The medial ends of the postcentral sulci typically arc around the partes marginales of the cingulate

FIG 3. *A–D,* Anatomic relationships of the parasagittal line on MR images. The composite representation (*A*) was traced from serial axial MR images (*B–D*). Labels as in Figures 1 and 2. Despite the differences in the scan angles and technology, MR images display the same anatomic relationships and the same alignments as CT scans do. Because the scan angle used for MR imaging is more horizontal, the partes marginales and adjacent sulci project further posteriorly on the serial axial images.

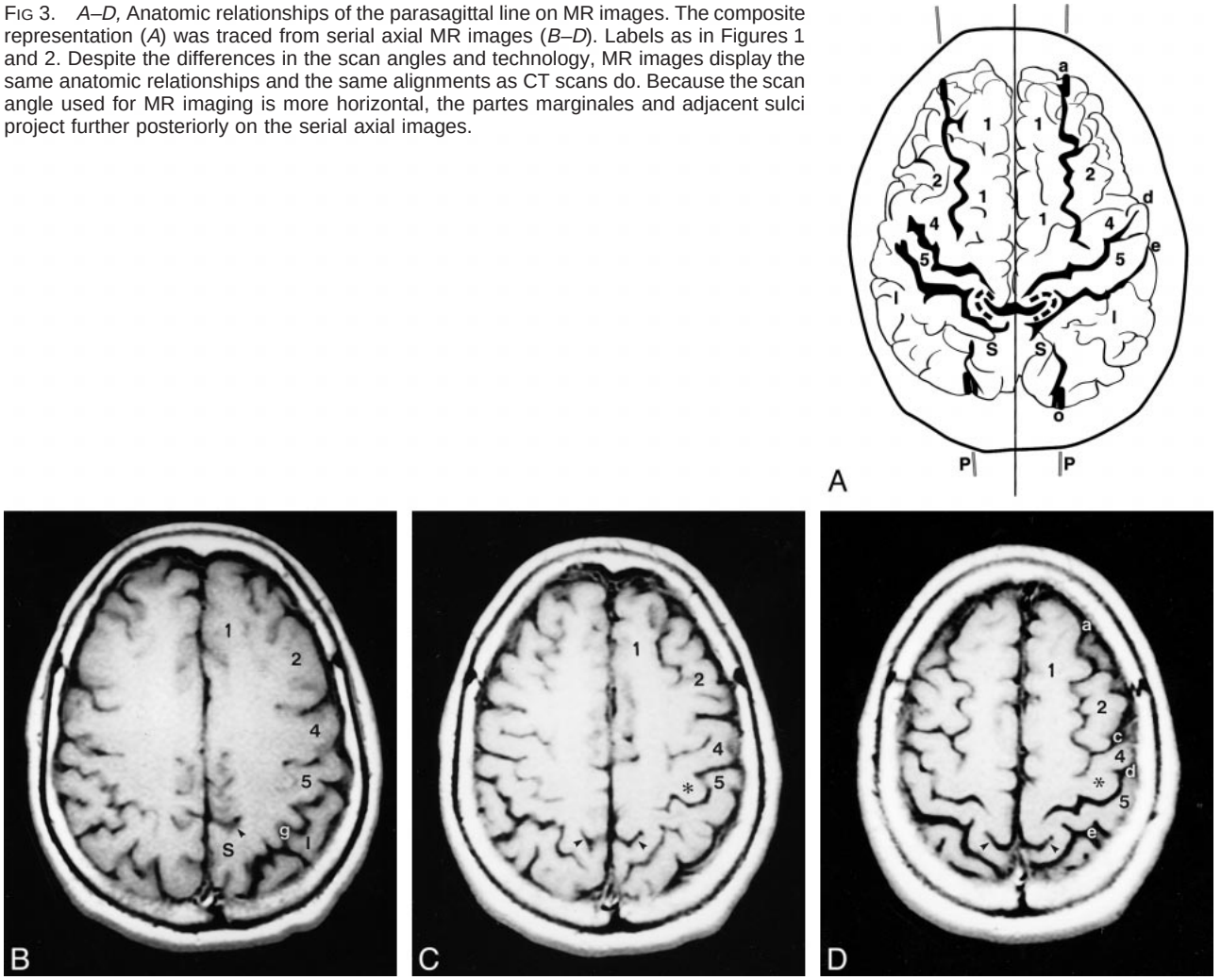

sulci to form postcentral parentheses (4). The postcentral parentheses were identifiable by CT in 194 (97%) of 200 hemispheres. The parentheses could not be discerned in two cases bilaterally and in two cases unilaterally. The postcentral parentheses lay medial to the parasagittal line in 54% of the 200 hemispheres, on the line in 32%, and lateral to the line in 11%. They were not seen in 3%. Defining malaligned as only those parentheses that fell lateral to the parasagittal line, the postcentral sulci were aligned in 86% of hemispheres, malaligned in 11%, and not seen in 3%. The malalignment affected three brains bilaterally and an additional 16 brains unilaterally (seven on the right and nine on the left).

The White Matter of the Pars Deflection (Figs 2–4)

The white matter that circumscribes the pars marginalis is designated the pars deflection (3). This narrow arc of white matter is situated between the medial cerebral cortex that curves around the lateral edge of the pars marginalis and the lateral cerebral cortex that lies just medial to the parenthesis of the postcentral sulci.

The pars deflection was seen by CT in all cases (100%). The pars deflection lay medial to the parasagittal line in 94%, on the line in 6%, and lateral to the line in none (0%) of the right hemispheres; it lay medial to the parasagittal line in 80%, on the line in 19%, and lateral to the line in 1% of the left hemispheres. Considering the 200 hemispheres together, the pars deflection lay medial to the parasagittal line in 87.5%, on the line in 12.5%, and lateral to the line in 0.5%. Defining malaligned as lateral to the parasagittal line, then the pars deflection was aligned in 99.5% and malaligned in 0.5% of the 200 hemispheres.

Deep invaginations of the partes marginales displaced the pars deflections laterally in 13% of hemispheres (Fig 4C and D). These laterally positioned pars deflections lay on the parasagittal line in 25 hemispheres and lateral to the line in one hemisphere. The displacement occurred more frequently on the left side than on the right side (20 left, six right); it was bilateral in four cases and unilateral in the rest. A definite correlation was

TABLE 1: Positions of anatomic structures with respect to the parasagittal line on CT (n = 200 hemipheres)

Structures on CT	Side	No.	Medial to the PSL	On the PSL	Lateral to the PSL	Not Seen	Percentage Aligned along the PSL	Percentage Malaligned
Superior frontal sulcus	R	100	0	100	0	0	100.0	0.0
	L	100	0	100	0	0		
	Total	200	0	200	0	0		
Precentral notch	R	100	1	77	21	1	97.5	0.5
	L	100	0	73	24	3		
	Total	200	1	150	45	4		
Hand-motor area (omega)	R	69	9	59	1	0	87.1	12.9
	L	78	4	69	5	0		
	Total	147	13	128	6	0		
Hand-motor area (epsilon)*	R	31	0	30	1	0	96.2	3.8
	L	22	0	21	1	0		
	Total	53	0	51	2	0		
Pars deflection	R	100	94	6	0	0	99.5	0.5
	L	100	80	19	1	0		
	Total	200	174	25	1	0		
Pars marginalis	R	100	95	2	0	3	95.5	1.5
	L	100	96	1	0	3		
	Total	200	197	3	0	0		
Postcentral parenthesis	R	100	59	27	10	4	86.0	11.0
	L	100	49	37	12	2		
	Total	200	108	64	22	6		
Subparietal sulcus	R	100	93	0	0	7	94.0	0.0
	L	100	95	0	0	5		
	Total	200	188	0	0	12		
Parietooccipital sulcus	R	100	97	1	0	2	98.0	0.0
	L	100	96	2	0	2		
	Total	200	193	3	0	4		
Intraoccipital sulcus	R	100	0	100	0	0	100.0	0.0
	L	100	0	100	0	0		
	Total	200	0	200	0	0		

Note.—PSL indicates parasagittal line.

* For the ϵ-shaped hand motor area only: medial to signifies that the PSL crosses entirely medial to the ϵ, on signifies that the PSL crosses the medial arc or the midpoint of the omega, lateral to signifies that the PSL crosses the lateral arc of the ϵ or that the whole ϵ lies lateral to the PSL.

found between the positions of the pars deflections and the postcentral parentheses. In the 25 cases in which the pars deflections were positioned on the parasagittal line, the surrounding postcentral parentheses were positioned lateral to the parasagittal line in 15 and on the line in the other 10. In the one case in which the left pars deflection was positioned lateral to the parasagittal line, the surrounding left postcentral parentheses also lay lateral to the line.

Viewed differently, the postcentral parentheses lay lateral to the parasagittal line in 11% of hemispheres: 10 right hemispheres and 12 left hemispheres. The pars deflections extended onto or lateral to the parasagittal line in four of these 10 right hemispheres (40%) and in all 12 of the left hemispheres (100%). The postcentral parenthesis extended onto the parasagittal line in 32% of hemispheres: 27 right hemispheres and 37 left hemispheres. The pars deflection also extended onto the parasagittal line in two (7.4%) of the 27 right hemispheres and in eight (21.6%) of the 37 left hemispheres. Thus, a lateral position of one structure suggested a lateral position of the other. The farther lateral the position of one, the greater the chance that both would lie laterally. Lateral position was more frequent on the left, and, when left, more frequently correlated with lateral position of other structures.

The Pars Marginalis (Figs 2–4)

The pars marginalis was visualized by CT in 97% of brains. The pars lay medial to the parasagittal line in 95% of right hemispheres and 96% of left hemispheres. The pars marginalis extended unusually far laterally onto the parasagittal line in only two (2%) of the right hemispheres and one (1%) of the left hemispheres. It never extended lateral to the parasagittal line. In both right hemispheres with laterally positioned partes marginales, the pars deflections lay on the parasagittal line and

TABLE 2: Positions of anatomic structures with respect to the parasagittal line on MR (n = 200 hemispheres)

Selected Structures on MR	Side	No.	Medial to the PSL	On the PSL	Lateral to the PSL	Not Seen	Percentage Aligned along the PSL	Percentage Malaligned
Superior frontal sulcus	R	100	0	100	0	0	100.0	0.0
	L	100	0	100	0	0		
	Total	200	0	200	0	0		
Precentral notch	R	100	4	93	2	1	94.5	4.0
	L	100	4	93	1	2		
	Total	200	8	186	3	3		
Hand-motor area (omega)	R	69	4	65	0	0	94.6	5.4
	L	78	3	74	1	0		
	Total	147	7	139	1	0		
Hand-motor area (epsilon)*	R	31	0	29	2	0	94.3	5.7
	L	22	0	21	1	0		
	Total	53	0	50	3	0		
Postcentral parenthesis	R	100	52	42	3	3	93.5	4.5
	L	100	38	55	6	1		
	Total	200	90	97	9	4		
Intraoccipital sulcus	R	100	0	100	0	0	100.0	0.0
	L	100	0	100	0	0		
	Total	200	0	200	0	0		

Note.—PSL indicates parasagittal line.

* For the ϵ-shaped hand motor area only: medial to signifies that the PSL crosses entirely medial to the ϵ, on signifies that the PSL crosses the medial arc or the midpoint of the ϵ, lateral to signifies that the pSL crosses the lateral arc of the ϵ or that the whole ϵ lies lateral to the PSL.

the postcentral parentheses lay on or lateral to the line. In the single left hemisphere with a laterally positioned pars marginalis, the left pars deflection and the left postcentral parenthesis both lay lateral to the parasagittal line. The pars marginalis was not seen in three right hemispheres and three left hemispheres, corresponding to one brain bilaterally and four other brains unilaterally. Defining malaligned as only those partes marginales that lay on or lateral to the parasagittal line, the partes marginales aligned with respect to the line in 98.5% and were malaligned laterally in 1.5%.

The Posterior Structures (Figs 2–4)

CT showed the SPS in 94% of cases. The SPS lay medial to the parasagittal line in all cases visualized. The posterior ends of the IPS converged toward the parasagittal line in all cases. The posterior portions of the IPS crossed medial to the parasagittal line in all but two hemispheres in which the visualized portion of the left IPS remained lateral to the line on all sections. In both these cases, the left postcentral parenthesis lay lateral to the parasagittal line and the left pars deflection lay on the line.

The POS were visualized in 98% of cases. They lay medial to the parasagittal line in all but three hemispheres (96.5%), and extended to the parasagittal line in two left hemispheres and one right hemisphere (1.5%), corresponding to one brain bilaterally and one brain unilaterally. Defining malaligned as a position lateral to the parasagittal line, then the POS was aligned in 98% of cases, malaligned in none (0%), and not visualized in 2%. The IOS lay on the parasagittal line in all cases, by definition.

Molding of the Occipital Bone (Figs 4C and 5)

In 152 (76%) of the 200 hemicalvaria, the inner table of the occipital bone showed subtle, vertically aligned bone ridges in relation to the posterior IPS and the IOS, unilaterally or bilaterally (Table 2). These bony ridges lay just medial to the IPS-IOS in 52 hemicalvaria (26%), at the IPS-IOS in 84 hemicalvaria (42%), and just lateral to the IPS-IOS in 16 hemicalvaria (8%).

Replication by MR Imaging

Precentral Sulcus.—MR imaging confirmed that the precentral notch was detectable in 98.5% of hemispheres, was aligned along or lateral to the parasagittal line in 94.5% of hemispheres, and was malaligned by more than 1.5 mm medial to the parasagittal line in 4% of hemispheres (Table 1B) (Fig 3).

The Hand-Motor Area of the Precentral Gyrus.—As with CT, the hand-motor area was identified by MR imaging in every case (100%), took the shape of a single omega (ω) in 147 of the 200 hemispheres (73.5%), and took the shape of an epsilon (ϵ) in 53 (26.5%) of the 200 hemispheres. On the right there were 69 ω's and 31 ϵ's, while on the left there were 78 ω's and 22 ϵ's. These two shapes were distributed as follows: bilateral ω, 61%; bi-

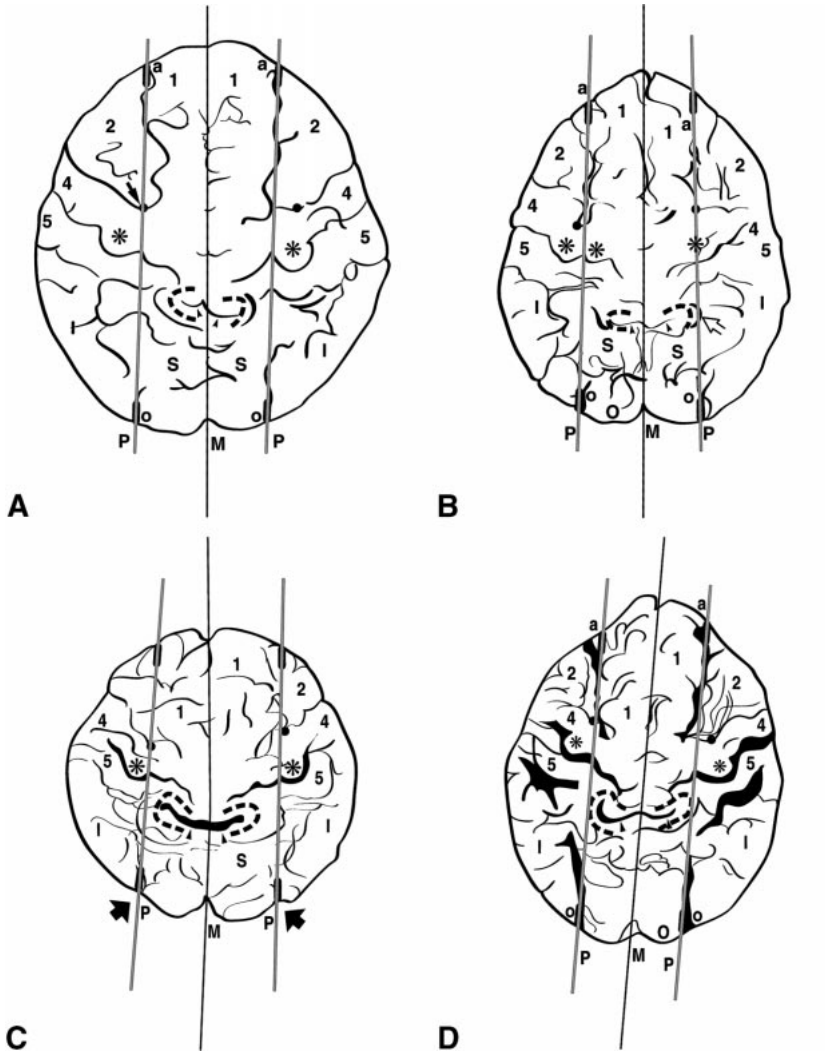

FIG 4. Parasagittal line. Limited anatomic diversity is seen on composite tracings from four different subjects. Labels as in Figures 1 and 2.

A, 27-year-old man. The anatomic alignment is stereotypical.

B, 42-year-old woman. The parasagittal line traverses the midpoint of a double arc ε-shaped hand-motor area (*small asterisks*) on the right. On the left, the medial edge of the single ω-shaped hand-motor area (*large asterisk*) lies medial to the parasagittal line, while the postcentral parenthesis (*open arrow*) lies on the line.

C, 13-year-old boy. Unusually deep extension of the right pars marginalis (emphasized in *black, arrowheads*) displaces the right pars deflection onto the parasagittal line. The precentral notches (*solid black circles*) and hand-motor areas (*asterisks*) align well with the parasagittal line. The *arrows* outside the brain contour at 5 o'clock and 7 o'clock indicate notches in the brain contour along the IOS, corresponding to the bony occipital ridges (see Fig 5).

D, 81-year-old woman. Very deep invagination of the partes marginales displace the pars deflections onto the parasagittal line bilaterally.

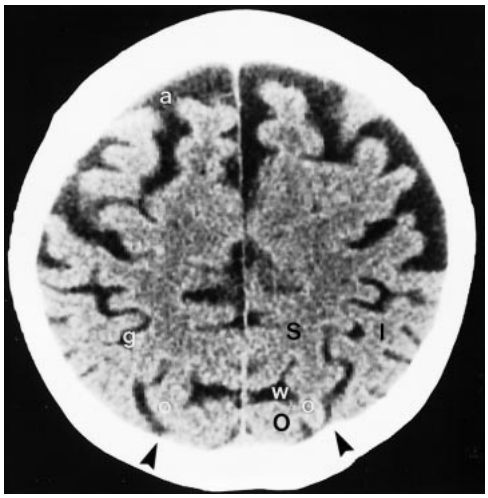

FIG 5. Molding of the occipital bone in a 76-year-old man. Normal scalloping of the inner table of the skull by the gyri situated to each side of the IPS-IOS commonly leaves small vertically oriented bony ridges (*arrowheads*) aligned along the parasagittal line. *I* = inferior parietal lobule, *large O* = superior occipital gyrus, *S* = superior parietal lobule, *a* = superior frontal sulcus, *g* = intraparietal sulcus, *small o* = intraoccipital sulcus, *w* = parietooccipital sulcus.

lateral ϵ, 14%; right ω, left ϵ 8%; and right ϵ, left ω 17%.

ω-Shaped Hand-Motor Area (n = 147): The parasagittal line crossed the precentral gyrus and the central sulcus just medial to the medial edge of the single ω-shaped hand-motor area in 94% of right hemispheres, 95% of left hemispheres, and 94.6% of the total 147 hemispheres with a single ω-shaped hand-motor area. The medial edge of the hand-motor area lay more than 1.5 mm medial to the parasagittal line in 5.8% of right hemispheres, 3.8% of left hemispheres, and 4.8% of the total 147 hemispheres. It lay more than 1.5 mm lateral to the parasagittal line in none of the right hemispheres (0%), in 1.3% of the left hemispheres, and in 0.7% of the total 147 hemispheres.

ϵ-Shaped Hand-Motor Area (n = 53): The parasagittal line crossed through the ϵ–shaped hand-motor area in 50 (94.3%) of 53 hemispheres. It crossed through the medial arc of the ϵ in 75.5% and crossed the midpoint of the ϵ in 18.9%; it never crossed through the lateral arc (0%). The entire ϵ of the hand-motor area lay more than 1.5 mm lateral to the parasagittal line in 5.7%.

Thus, the hand-motor area aligned along the parasagittal line in 94.6% of 147 hemispheres with an ω-shaped hand-motor area and in 94.3% of 53 hemispheres with an ϵ-shaped hand-motor area. It was malaligned medial to the parasagittal line in 2.7% of hemispheres with an ω-shaped hand-motor area and in 0% with an ϵ-shaped hand-motor area. It was malaligned lateral to the parasagittal line in 0.7% of the ω-shaped hand-motor areas and in 5.7% of the epsilon-shaped hand-motor areas.

The Parenthesis of the Postcentral Sulcus (1.0-mm Criterion).—MR imaging confirmed that the postcentral parentheses were detectable in 98% of hemispheres, but could not be discerned in one case bilaterally (1%) and in two cases unilaterally (1%). The postcentral parentheses lay medial to (45%), on (48.5%), or lateral to (4.5%) the parasagittal line in 98% of hemispheres, and were not identified in 2% of hemispheres. Defining malaligned as only those positions lateral to the parasagittal line, then the postcentral parentheses were aligned in 93.5% of all hemispheres and were malaligned in only 3% of right hemispheres, 6% of left hemispheres, and 4.5% of all hemispheres.

The postcentral parentheses lay medial to the parasagittal line bilaterally in 23 brains, on the line (± 1.0 mm) bilaterally in 27 brains, and lateral to the line bilaterally in one brain (1%). The postcentral parentheses were distributed asymmetrically medial to the parasagittal line on one side but on the line on the other side in 39 brains (39%). In the others, the parentheses showed mixed alignment: medial/not detectable in two brains, medial/lateral in three brains, and lateral/on in four brains.

Discussion

The cause of cortical folding and the genesis of specific gyri and sulci remain undetermined (16–20). Three major hypotheses have been advanced (16, 19): 1) pleating of the cortex in response to extrinsic compressions by adjacent limiting structures (Clark [16], cited in Richman et al [17]), 2) folding of the cortex along the boundaries between different cytoarchitectonic fields (17), and 3) folding of the cortex purely in response to intrinsic intracortical stresses that are generated by differing rates of growth of the individual cortical layers I through VI (21). Working with developing sheep brains, Barron ablated much of the central hemisphere, including the central white matter, after the period of neuronal migration but before the appearance of convolutions. Despite the extensive ablations, resultant disconnections, and alterations in the adjacent constraints and compressions, all the animals had gyri and sulci of essentially normal size and configuration at term (21). These findings suggest that intrinsic intracortical stresses may be the most significant. Persistence of the expected alignment of the parasagittal line despite calvarial elongation and biparietal compression from premature sagittal synostosis (Fig 6) would support this concept. Other factors are also likely to play a role, since the gyral-sulcal pattern of monozygotic twins is not identical, only similar (20).

The study data indicate that the parasagittal line, which extends between the SFS anteriorly and the IOS posteriorly, traverses anatomically reproducible areas, including a notable alignment with the medial edge of the hand-motor area (Figs 2–4). Characteristically, the parasagittal line runs through the SFS, through or just medial to the precentral notch, along the medial edge of the hand-motor area, lateral to the pars marginalis, on or lateral to the pars deflection, on or lateral to the postcentral parentheses, lateral to the SPS and POS, and along the posteriormost IPS-IOS. The very limited variation in the anatomic relationships of the parasagittal line validates its use as an anatomic landmark.

Because the parasagittal line has a fixed relationship to brain structures, it also marks sites of brain function. From anterior to posterior, these include the frontal eye fields, the hand-motor areas, the vibration sensation for the hand, and the posterior parietal eye fields. The frontal eye fields disengage fixation and trigger saccades for intentional exploration of the visual environment; for example, saccades to visible targets, to remembered target locations, and to the location where it is predicted that a target will reappear (21). Paus (22) and Luna et al (23) have shown that the human frontal eye fields lie in the precentral sulcus and/or deep in the adjacent caudalmost SFS; that is, along the parasagittal line, not in Brodmann area 8, as was previously thought. Thus, the frontal eye fields fall along the parasagittal line. Hand-motor function has been localized to the knob along the posterior face of the precentral gyrus (10–12). This hand-motor area lies at or immediately lateral to the parasagittal line. Vibration sensation in the hand lies along the concave anterior face of the postcentral gyrus immediately posterior to the knob for the hand-motor area (24), also at and immediately lateral to the parasagittal line. The posterior parietal eye field triggers saccades made reflexively upon the sudden appearance of visual targets (21) or for controlling saccadic eye movements to target locations (25). Kawashima et al (25) have shown that the posterior parietal eye fields lie within the posterior IPS. The posterior parietal eye fields, then, also appear to align along the posterior parasagittal line.

By choice, the parasagittal line was defined to coincide with the major longitudinally oriented sulci of the high convexity: the SFS and the IOS. Further analysis revealed that the parasagittal line also aligns along numerous short segments of, notches in, and deflections of the transversely oriented high convexity sulci; specifically, the notch in the precentral sulcus, the inscription in the central sulcus at the hand-motor area, the parentheses of the postcentral sulci, and the posteriorly converging seg-

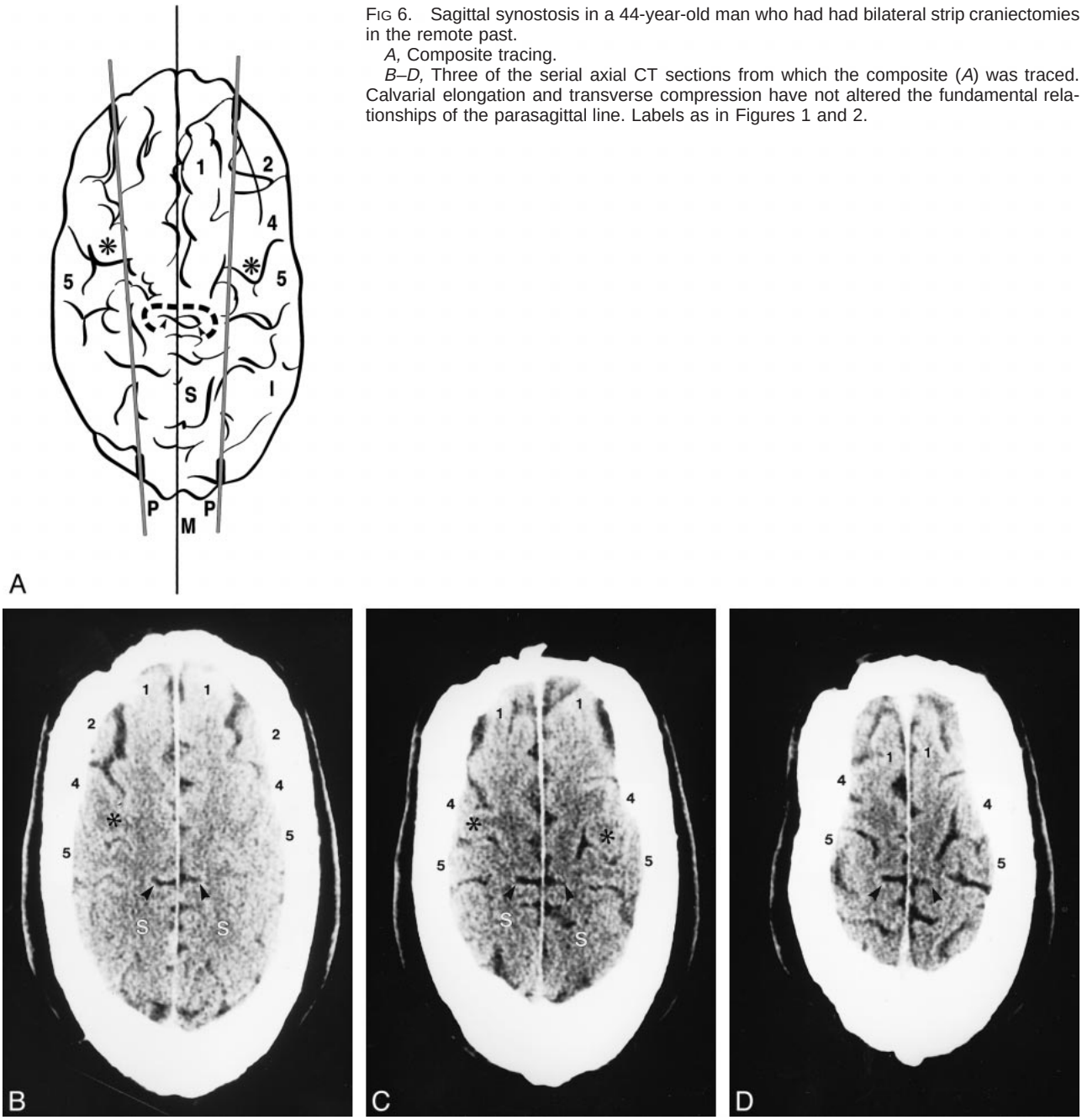

FIG 6. Sagittal synostosis in a 44-year-old man who had had bilateral strip craniectomies in the remote past.

A, Composite tracing.

B–D, Three of the serial axial CT sections from which the composite (*A*) was traced. Calvarial elongation and transverse compression have not altered the fundamental relationships of the parasagittal line. Labels as in Figures 1 and 2.

ments of the IPS-IOS (Figs 1–4). Thus, the parasagittal line may delineate a natural zone for folding and pleating of the cerebral cortex longitudinally.

The parasagittal line appears to delimit the lateral border of a parasagittal strip of tissue composed of the high convexity–parasagittal portions of the superior frontal gyrus, precentral and postcentral gyri, the uppermost superior parietal lobule, and the superior occipital gyrus. These areas represent the convexity surfaces of those parasagittal gyri that extend over the cerebral margin onto the flat medial surface of the brain, where they are renamed the medial frontal gyrus (corresponding to the superior frontal gyrus), the paracentral lobule (corresponding to the precentral gyrus and most of the postcentral gyrus), the precuneus (corresponding to the superior parietal lobule), and the cuneus (corresponding to the superior occipital gyrus).

The parasagittal line also divides the medial surface and its sulci from the convexity surface and its sulci. That is, the parasagittal line appears to demarcate the deepest (lateral) extent of the sulci that indent the medial surface of the brain; specifically, the paracentral sulci, the partes marginales, the SPS, and the POS (Figs 1–4). At the mid-high convexity, the parasagittal line simultaneously delimits the medial extent of the lateral sulci that indent the convexity surface of the brain (Figs 1–4). Thus, the parasagittal line appears to serve as a

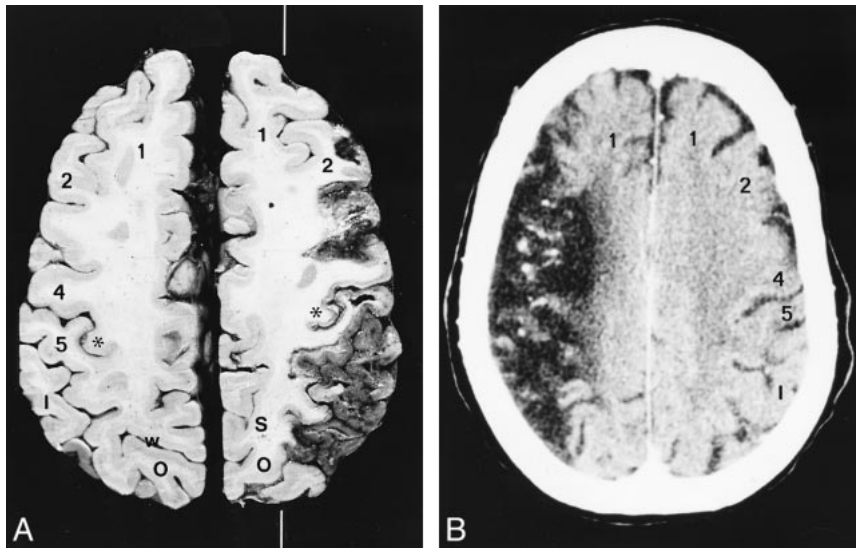

FIG 7. The parasagittal line and cerebral infarction. Middle cerebral artery infarctions in two subjects.

A, Anatomic section. The *white line* indicates the position of the parasagittal line. (Case courtesy of Drs. Anne Osborne and Tessa Hedley-Whyte.)

B, Noncontrast CT scan. In the supraventricular sections, the medial borders of infarctions tend to align along the parasagittal line.

natural line of demarcation between medial and lateral portions of the brain, separated by a line of longitudinal pleating.

Since the cerebral vasculature condenses onto the brain surface in relation to the unpleated immature brain (26) and then folds with the brain surface as the cortex matures, the parasagittal line also tends to demarcate the medial portion of the cortex typically supplied by the anterior and posterior cerebral arteries from the lateral portion typically supplied by the middle cerebral arteries (Fig 7). The parasagittal line may, therefore, approximate the position of the parasagittal watershed between the anterior and middle cerebral arteries and the posterior and middle cerebral arteries. Since the precise positions of the parasagittal watersheds vary in ways that are notoriously difficult to describe simply (27), the reproducible parasagittal line may provide a landmark useful for describing variations in individual vascular territories, the medial-lateral extent of infarctions and, perhaps, the zones in which collateral flow is most likely to rescue ischemic tissue. This subject will be addressed in a forthcoming publication.

Certain technical constraints may have introduced errors into the analysis of the parasagittal line. In this study, the sulci were traced onto one surface directly from the hard-copy images to ensure accurate reproduction of the configurations of the sulci. The exact positions of the sulci proved to be subject to greater error, since the tracing paper was necessarily moved from section to section. Indeed, in many patients with slight head cant or falx asymmetry, the paper was deliberately shifted left-right or anterior-posterior to maintain the anatomic integrity of the image as the patient's midline shifted subtly from slice to slice. Petalia, a term that has been used to describe the exaggeration of one occipital lobe and the contralateral frontal lobe with skew deviation of the midline (15), is especially associated with significant deviation of the falx away from the midline to either or both sides, and was a real consideration in this study. The asymmetries associated with petalia could, however, be compensated for successfully by using the curved falx as its own midline. That is, the curve of the falx on one section was traced onto the flat surface to establish the expected curve of the patient's own midline. All subsequent sections were then aligned to the first by matching the curve of the falx in that section to the curve drawn from the first section (Fig 4C).

Identifying the SFS and the IOS was difficult at times. First, because these sulci curve and tilt from medial to lateral as they course through the different sections, and second, because the superior frontal gyrus is partially, incompletely subdivided into medial and lateral portions by the medial frontal sulci (100% left, 100% right) (8), while the middle frontal gyrus may be similarly partially subdivided by the middle frontal sulcus (84% left, 88% right) (8). In such cases, one must choose from among multiple parallel frontal sulci which sulcus to designate the SFS for drawing the parasagittal line.

Posteriorly, similar difficulty was encountered in choosing the IOS. On CT scans, a subtle point of bone was present where the IOS reached the inner table in 76% of cases. Presumably this represents the line of bone that remains between the digital impressions created medial to the line by the superior occipital gyrus and lateral to the line by the middle occipital gyrus (9). When present, the posterior point helped to identify the IOS (Fig 5).

On occasion, choosing which portion of the precentral gyrus should be designated the hand-motor area and determining whether to classify the hand-motor area as a single omega (ω) or as a double-hump epsilon (ϵ) proved more intuitive than would be desired. In nearly every case, however, the complete pattern formed by all the sulci and gyri permitted ready identification of the hand-motor area (4). The relationship between the hand-motor area and the parasagittal line can therefore serve as an

additional check on the region to be designated the hand-motor area.

In the future, computer manipulation of brain surfaces (28, 29) should permit ready display of the parasagittal line in patients, extension of the parasagittal line into a three-dimensional parasagittal plane, and description of the parasagittal line in Talairach space (30), thus providing a further guide to analyzing disease processes in three-dimensional reformations.

Conclusion

Detailed analysis documents that a parasagittal line drawn through the SFS anteriorly and IOS posteriorly has reproducible relationships to the adjacent gyri and sulci. This parasagittal line may then serve as a landmark for describing anatomy and abnormalities. The relationships of the parasagittal line to the deep longitudinal sulci and to abrupt deflections in transverse high convexity sulci suggest that this line may correspond to a line of longitudinal pleating of the cortex. The relationships of the line to structures supplied by the three major cerebral arteries suggest the need to assess the application of the parasagittal line to defining vascular territories, watersheds, and cerebral infarctions.

1. Naidich TP, Brightbill TC. **The intraparietal sulcus: a landmark for localization of pathology on axial CT scans.** *Int J Neuroadiol* 1995;1:3–16
2. Naidich TP, Brightbill TC. **The pars marginalis, II: a "bracket" sign for the central sulcus in axial plane CT and MRI.** *Int J Neuroradiol* 1996;2:3–19
3. Naidich TP, Brightbill TC. **The pars marginalis, II: the pars deflection sign, a white matter pattern for identifying the pars marginalis in axial plane CT and MRI.** *Int J Neuroradiol* 1996; 2:20–24
4. Naidich TP, Brightbill TC. **Systems for localizing fronto-parietal gyri and sulci on axial CT and MRI.** *Int J Neuroradiol* 1996;2: 313–338
5. Valente M, Naidich TP, Abrams KJ, Blum JT. **Differentiating the pars marginalis from the parieto-occipital sulcus in axial computed tomography sections.** *Int J Neuroadiol* 1998;4:105–111
6. Naidich TP, Valavanis AG, Kubik S. **Anatomic relationships along the low-middle convexity, I: normal specimens and magnetic resonance imaging.** *Neurosurgery* 1995;36:517–532
7. Naidich TP, Valavanis AG, Kubik S, Taber KH, Yasargil M. **Anatomic relationships along the low-middle convexity, II: lesion localization.** *Int J Neuroradiol* 1997;3:393–409
8. Ono H, Kubik S, Abernathy C. ***Atlas of Cerebral Sulci.*** Stuttgart: Thieme; 1990
9. Duvernoy H. ***The Human Brain: Surface, Three Dimensional Sectional Anatomy and MRI.*** New York: Springer;1991
10. Yousry TA, Schmid UD, Alkadhi H, et al. **Localization of the motor hand area to a knob on the precentral gyrus: a new landmark.** *Brain* 1997;120:141–157
11. Yousry TA, Schmid UD, Jassoy AJ, et al. **Topography of the cortical motor hand area: prospective study with functional MR imaging and direct motor mapping at surgery.** *Radiology* 1995;195:23–29
12. Yousry TA, Fesl G, Buttner A, Noachtar S, Schmid UD. **Heschl's gyrus: anatomic description and methods of identification on magnetic resonance imaging.** *Int J Neuroradiol* 1997;3:2–12
13. Meyer J, Roychowdhury S, Russell E, Callahan C, Gitelman D, Mesulam MM. **Location of the central sulcus via cortical thickness of the precentral and postcentral gyri on MR.** *AJNR Am J Neuroradiol* 1996;17:1699–1706
14. Ebeling U, Steinmetz H, Huang Y, Kahn T. **Topography and identification of the inferior precentral sulcus in MR imaging.** *AJNR Am J Neuroradiol* 1989;10:937–942
15. LeMay M. **Asymmetries of the skull and handedness: phrenology revisited.** *J Neurol Sci* 1977;32:243–253
16. Le Gros Clark WE, Medawar PB, eds. ***Essays on Growth and Form Presented to Darcy Wentworth Thompson.*** London: Oxford University Press;1945:1–22
17. Richman DP, Stewart M, Hutchinson JW, Caviness VS Jr. **Mechanical model of brain convolutional development: pathologic and experimental data suggest a model based on differential growth within the cerebral cortex.** *Science* 1975;189:18–21
18. Prothero JW, Sundsten JW. **Folding of the cerebral cortex in mammals: a scaling model.** *Brain Behav Evol* 1984;24:152–167
19. Zilles K, Armstrong E, Schleicher A, Kretschmann H-J. **The human pattern of gyrification in the cerebral cortex.** *Anat Embryol* 1988;179:173–179
20. Biondi A, Nogueira H, Dormont D, et al. **Are the brains of monozygotic twins similar? A three-dimensional MR study.** *AJNR Am J Neuroradiol* 1998;19:1361–1367
21. Barron DH. **An experimental analysis of some factors involved in the development of the fissure pattern of the cerebral cortex.** *J Exp Zool* 1950;113:553–581
22. Paus T. **Location and function of the human frontal eye field: a selective review.** *Neuropsychologia* 1996;34:475–483
23. Luna B, Thulborn KR, Strojwas MH, et al. **Dorsal cortical regions subserving visually guided saccades in humans: an fMRI study.** *Cereb Cortex* 1998;8:40–47
24. Rumeau C, Tzourio N, Murayama P, et al. **Location of hand function.** *AJNR Am J Neuroradiol* 1994;15:567–572
25. Kawashima R, Naitoh E, Michikazu M, et al. **Topographic representation in human intraparietal sulcus of reaching and saccade.** *Neuroreport* 1996;7:1253–1256
26. Naidich TP, Grant JL, Altman N, et al. **The developing cerebral surface: preliminary report on the patterns of sulcal and gyral maturation: anatomy, ultrasound, and magnetic resonance imaging.** *Neuroimaging Clin North Am* 1994;4:201–240
27. Van der Zwan A, Hillen B, Tulleken CAF, Dujovny M, Dragovic L. **Variability of the territories of the major cerebral arteries.** *J Neurosurg* 1992;77:927–940
28. Greitz T, Bohm C, Holte S, Eriksson L. **A computerized brain atlas: construction, anatomical content and some applications.** *J Comput Assist Tomogr* 1991;15:26–38
29. Vanier M, Roch Lecours A, Ethier R, et al. **Proportional localization system for anatomical interpretation of cerebral computer tomograms.** *J Comput Assist Tomogr* 1985;9:715–724
30. Talairach J, Tournoux P. ***Co-planar Stereotaxic Atlas of the Human Brain: 3-Dimensional Proportional System, an Approach to Cerebral Imaging.*** Stuttgart: Thieme Medical; 1998